Nearest-neighbor distance distributions and self-ordering in diffusion-controlled reactions. II. $A+B$ simulations

Panos Argyrakis
Department of Physics 313-1, University of Thessaloniki, GR-54006 Thessaloniki, Greece and Department of Chemistry, University of Michigan, Ann Arbor, Michigan 48109-1055

Raoul Kopelman
Department of Chemistry, University of Michigan, Ann Arbor, Michigan 48109-1055
(Received 8 March 1989)

Monte Carlo simulations of transient, diffusion-controlled $A+B\rightarrow 0$ reactions are performed on one-, two-, and three-dimensional Euclidean lattices and on a fractal lattice (two-dimensional critical percolation cluster). The particle distributions are analyzed by partial nearest-neighbor distance distributions (NNDD), taxicab NNDD, and linearized NNDD. Comparisons are made with NNDD and interparticle distributions of the $A+A\rightarrow 0$ and $A+A\rightarrow A$ reactions (extending some of the simulations of the preceding paper [Phys. Rev. A **41**, 2113 (1990)]), revealing some empirical connections. The aggregation of like particles and the segregation of unlike particles are monitored in time, for the various diffusion topologies. The relations between the partial NNDD, the microscopic and mesoscopic ordering, and the global rate laws are discussed.

I. INTRODUCTION

Paper I of this series[1] exhibited the self-ordering in transient $A+A$ reactions constrained to low-dimensional spaces: one-dimensional and two-dimensional lattices as well as square-lattice critical percolation clusters. The interparticle distribution function ("gaps") and the nearest-neighbor distance distributions (NNDD) were the tools for analysis. The first one (gap) has been used[2] in analytic approaches (in one-dimensional continuum only), but has as a drawback that it is limited to one dimension. The equivalent NNDD can be generalized to any dimension (even fractal ones) and has been used with a taxicab ("Manhattan") metric.[3] (The taxicab geometry is a non-Euclidean geometry, named for its applicability to models of urban geography for the case in which square networks represent the interconnecting streets, e.g., for the Manhattan Borough of the City of New York.) This approach considers particle distances as the sum of their Cartesian coordinate differences. It has been shown[1] for the $A+A$ reactions that the NNDD are good order indicators, that they scale with reactant concentration, and that there is a simple relation between the NNDD and the global rate laws. The surprising differences in the NNDD of $A+A\rightarrow 0$ and $A+A\rightarrow A$ reactions have been shown to diminish with increasing dimensionality.

In this paper we extend our investigation to $A+B$ reactions and to higher dimensionality (cubic lattices) and we add some methods for particle distribution characterization. The somewhat surprising results reveal empirical connections between the $A+A$ and the $A+B$ reactions. While the aggregation of like-like particles (AA,BB) is rapid, this is not followed by a rapid segregation of the AB particles. The aggregation and segregation are monitored via *partial* NNDD functions. The partial AB NNDD functions are actually very similar to the NNDD of the $A+A$ reactions, particularly for the annihilation ($A+A\rightarrow 0$) reaction in one dimension. These similarities are preserved in the higher dimensions (including $d=3$), even though the differences between the annihilation and the fusion ($A+A\rightarrow 0$) reactions become smaller with increasing dimensionality.

To make the simulation of the particle distributions also feasible in three dimensions, we use a linearized (linear cuts) NNDD approach (explained in Sec. II). This reveals the local, microscopic ordering that takes place in three dimensions (creating local "black holes").

We also attempt to fit empirically some of the NNDD functions, with partial success. These empirical fits are also tested against a *local-rate-law formalism.*

II. METHOD OF CALCULATIONS

The mechanisms for the chemical reaction calculations are similar to those described in paper I. Briefly, particles with two distinct identities are placed randomly on lattices of one-dimensional, two-dimensional, and three-dimensional topologies. No two particles of any type are allowed to occupy the same site simultaneously. Diffusional motion is simulated as random walks by all particles, in the spirit of all previous work on this subject.[1-4] If particles of opposite type are found to occupy the same site at any one time, they are annihilated, signifying a chemical reaction. Two A or two B particles are not allowed to collide or react. The search for the nearest neighbors is performed in the same method as previously. The breadth-first search (BFS) technique[5] is also used here for locating the nearest neighbor in the random percolating clusters. The simulations were performed on various Microvax Computers. Key numbers are given in Table I.

The distributions in two dimensions and three dimen-

TABLE I. Kinetic and distribution data. N is the number of particles of each component.

t	$\langle r(AA)\rangle$	$\langle r(AB)\rangle$	$\langle r(PP)\rangle$	N
		One dimensional		
0	10.26	10.24	5.26	500
100	18.04	34.30	11.01	246.5
500	24.39	67.40	16.02	164.3
1000	28.15	92.30	19.05	136.4
2000	32.58	127.40	22.75	112.8
5000	39.73	195.10	28.83	87.7
		One-dimensional gap		
0	9.96	9.98		500
100	16.94	26.62		246.5
500	24.58	46.61		164.3
1000	29.36	60.54		136.4
		Two dimensional		
0	2.84	2.84	2.04	2000
100	5.78	8.52	4.54	404.3
500	9.26	17.35	7.50	142.9
1000	11.46	23.59	9.39	89.7
2000	14.04	30.64	11.92	55.5
		Two-dimensional p_c		
0	5.15	5.14		520.2
500	10.67	23.76		131.3
		Three dimensional		
0				3200
10				1795
20				1284
50				707
100				411

sions for the linear neighbors are obtained as follows: Each direction (front-back, left-right, up-down, as the case may be) is searched separately. For the two-dimensional lattices first all rows are searched, one by one. Neighbors only on the same row are recorded, while all other particles are being ignored. Cyclic boundary conditions are used in all directions. In many instances no such neighbors are found, in which case there is no contribution to the distribution function. After all rows have been searched, the columns are treated similarly and added to the previous function to improve on the statistics. Finally, for the three-dimensional lattices the same is done to the heights. We note that the search obeys the cyclic boundary conditions, but is terminated at $r=l$, where l is the linear dimension of the lattice (200 for square lattice, 40 for cubic lattice).

III. RESULTS AND DISCUSSION

Figure 1 shows the NNDD distributions for $A+B\rightarrow 0$ on a one-dimensional lattice. The initial ($t=0$) distribution is the random (Hertz) Poissonian distribution.[1,6,7] After 1000 reaction steps the overall particle-particle (PP) distribution is still essentially the same (random). However, there is significant structure visible in the partial distribution functions (the given $t=1000$ curves differ little from $t=100$ and 2000 curves). The like-like particle partial NNDD (AA as well as BB) is "compressed" into a superexponential shape while the like-unlike (AB) partial NNDD is Wigner-like,[8,9] i.e., with a well-developed maximum. This is even more pronounced for the interparticle (gap) AB partial distribution. We note that the AB gaps are all located at reaction interfaces, while the AB NNDD has contributions from "shielded" particles (e.g., in an AAB cluster, both the short and the long AB distance contribute to the AB NNDD, while only the short one contributes to the AB gap). Figure 2

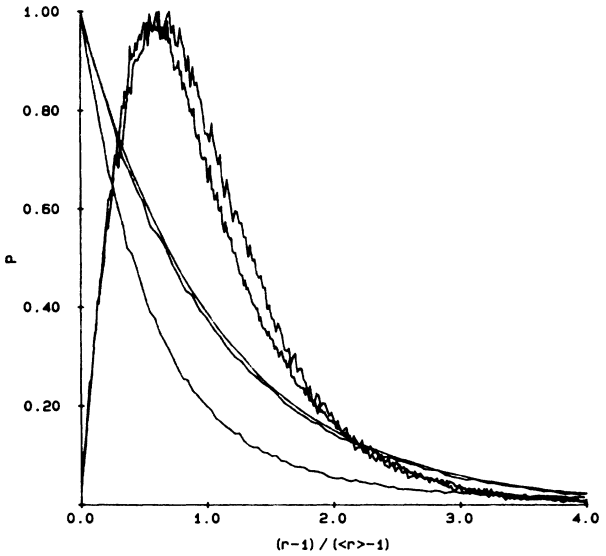

FIG. 1. NNDD for one-dimensional $A+B\rightarrow 0$ reactions. Shown are the $t=0$ curve (random distribution, same for all cases) and the $t=1000$ like-like (AA), like-unlike (AB), and particle-particle (PP) distributions for nearest-neighbor distances (2000 runs). Also shown is the distribution for gaps for the like-unlike case (5000 runs). Total number of lattice sites is 10000 and the initial ($t=0$) concentration is 0.05 for A and 0.05 for B (0.1 for P).

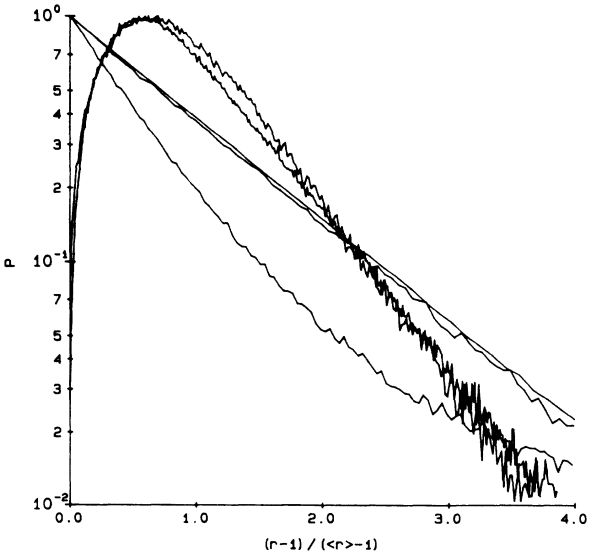

FIG. 2. Same as Fig. 1 in semi-log form.

is a semilog presentation, emphasizing the non-Poissonian nature of all the partial NNDD's.

Figure 3 compares the above AB NNDD to the NNDD of an $A + A \rightarrow 0$ reaction (paper I), under similar conditions (same lattice, $\rho_0 = 0.05$, $t = 1000$). It is obvious that the two distributions are essentially identical (accidentally?). We note that presently there is no analytical form available for the $A + A \rightarrow 0$ NNND (or gap). We only know that in the large distance limit the NNDD decays exponentially (see paper I), that for the short distance limit it rises linearly (paper I) and that overall the skewed-exponential form ($xe^{-\alpha x}$) is an approximate, but crude fit (paper I), as can be seen from Fig. 4.

Figure 5 gives the $A + B \rightarrow 0$ NNDD and partial NNDD functions for a two-dimensional (square) lattice. The AA partial NNDD is significantly shifted (compressed) relative to the $t = 0$, random (taxicab Hertz) distribution (which is practically the same as the Hertz distributions of paper I). On the other hand, the AB partial NNDD is practically indistinguishable from the Hertz NNDD, at this level of simulation. The particle-particle (overall) NNDD appears to be nonrandom, and in between the AA and AB distributions (as expected). Based on the present quality of simulations, the AB distribution may or may not differ from the two-dimensional $A + A$ reaction distributions (paper I). We further note that the two-dimensional random (Hertz) NNDD has a skewed Gaussian form (paper I), which may or may not also be the case for the AB NNDD, but is certainly not the case for the AA NNDD (and PP NNDD).

Figure 6 gives the $A + B \rightarrow 0$ partial NNDD curves for the critical percolation cluster on a square lattice. The AA partial NNDD differs significantly from the $t = 0$ (random) NNDD while the AB partial NNDD may differ

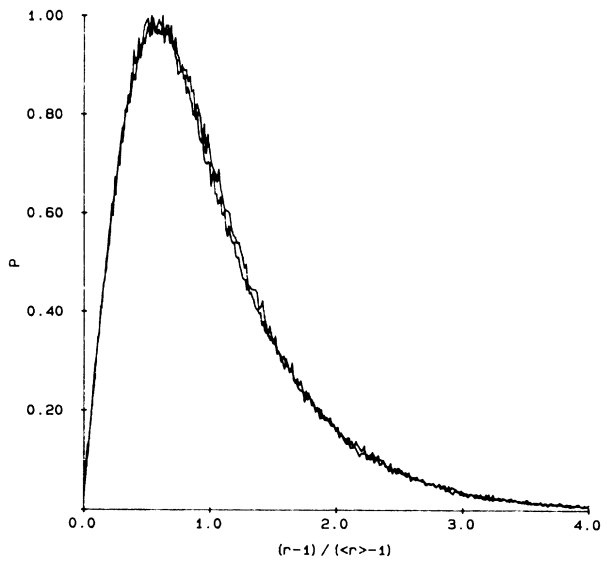

FIG. 3. Comparison graph of the $A + A \rightarrow 0$ and $A + B \rightarrow 0$ reactions in one-dimensional space. The $A + A \rightarrow 0$ NNDD data ($t = 1000$) is taken from paper I while the AB NNDD is taken from Fig. 1.

from it only slightly (and is shifted in the opposite direction?). This "fractal kinetics" case, with a fractal dimension of 1.896 and a spectral (fracton) dimension of 1.333 appears, indeed, to be in between the one-dimensional and two-dimensional situations ($d = 1$ and 2, respectively). The AB partial NNDD is also quite similar (within the simulations uncertainties) to the $A + A$ NNDD curves (paper I).

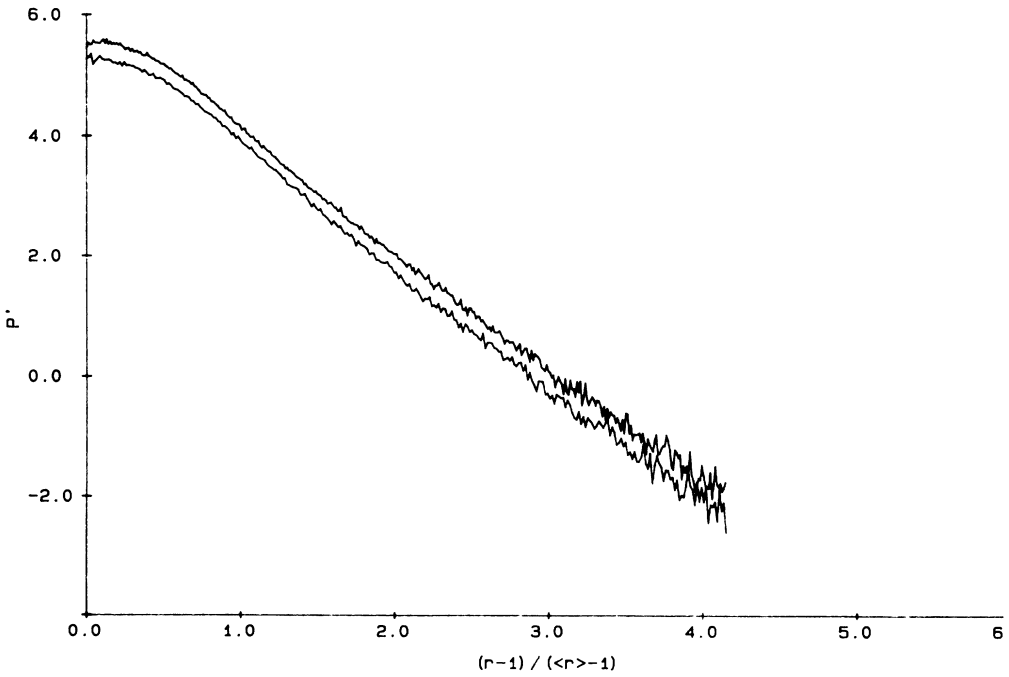

FIG. 4. Plot of P' [defined as $\ln P(r) - \ln(r/\langle r \rangle) + \ln\langle r \rangle$] vs $(r-1)/(\langle r \rangle - 1)$ for the data of Fig. 3.

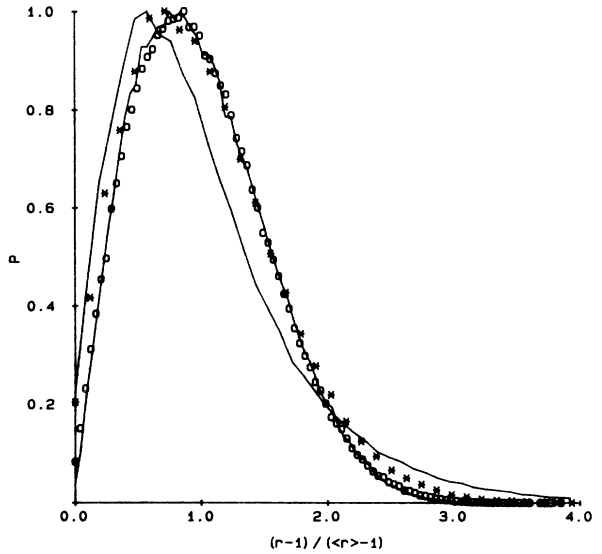

FIG. 5. Plot of the NNDD for the two-dimensional $A+B\rightarrow 0$ reactions ($t=1000$). Similar curves as in Fig. 1. 1000 runs on a 200 × 200 lattice. Same initial densities as in Fig. 1. Left curve, AA; right curve, AB; circles, $t=0$ (random); stars, PP.

In order to make comparisons with the three-dimensional (cubic) lattices one would like to perform reaction simulations followed by a three-dimensional NNDD (taxicab) analysis. Such an analysis is computation intensive. We chose instead to apply a "linearized NNDD" analysis (see Sec. II). We tested it first on the two-dimensional (square) lattice. The results for the two-dimensional $A+B$ reaction are given in Fig. 7. We

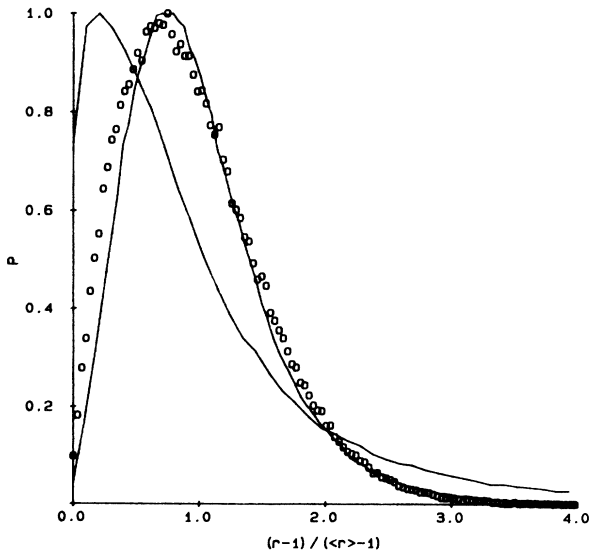

FIG. 6. Plots of the NNDD for the two-dimensional $A+B\rightarrow 0$ reactions on percolation clusters exactly at the critical percolation threshold. 1000 runs, $t=500$, $\rho_0=0.05$. Left curve, AA; right curve, AB; circles, $t=0$ (random).

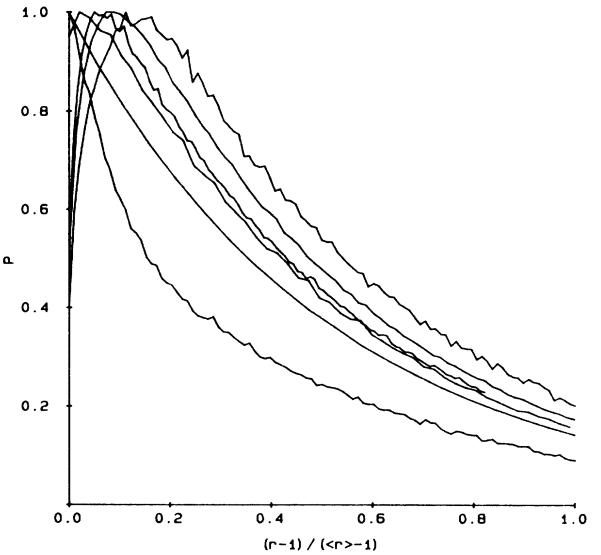

FIG. 7. Linearized NNDD (see text) for two-dimensional $A+A$ and $A+B$ reactions. All curves are for $t=100$ steps, except the $t=0$ (random distribution, smooth curve). Top to bottom (right-hand side): (1) $A+B\rightarrow 0$, AB NNDD; (2) $A+A\rightarrow A$; (3) $A+A\rightarrow 0$; (4) $A+B\rightarrow 0$, PP NNDD; (5) $t=0$ random NNDD; (6) $A+B\rightarrow 0$, AA NNDD. 5000 runs on 200×200 lattice with initial density $\rho_0 = 0.05$ for each component. $\langle r \rangle$ is given by ρ^{-1}.

discuss first the random ($t=0$) distribution. Due to the finite size of the lattice (200 × 200), the x axis normalization is not reliable, as $\langle r \rangle$ is of the size of the lattice (this was not so for the one-dimensional lattices and for the taxicab distances in the two-dimensional lattice). It is only by consulting Fig. 8 that we corroborate the Poissonian (exponentially decaying) functional form of the random (Hertz) NNDD along a linear "cut." Qualitatively, however, Fig. 7 gives the expected information

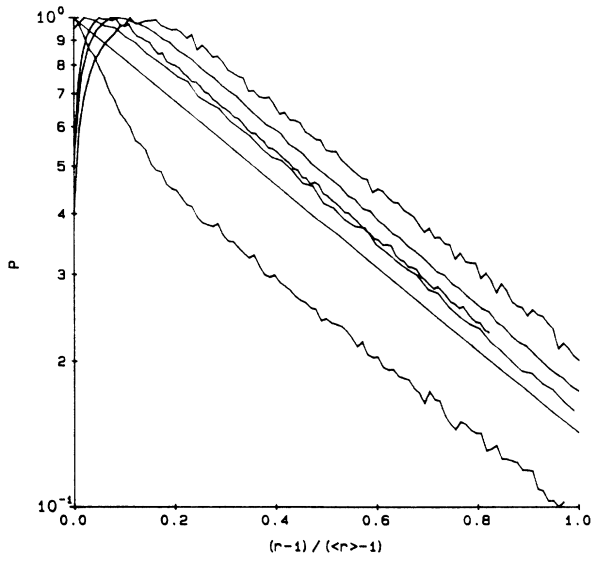

FIG. 8. Semilog plot of Fig. 7 data.

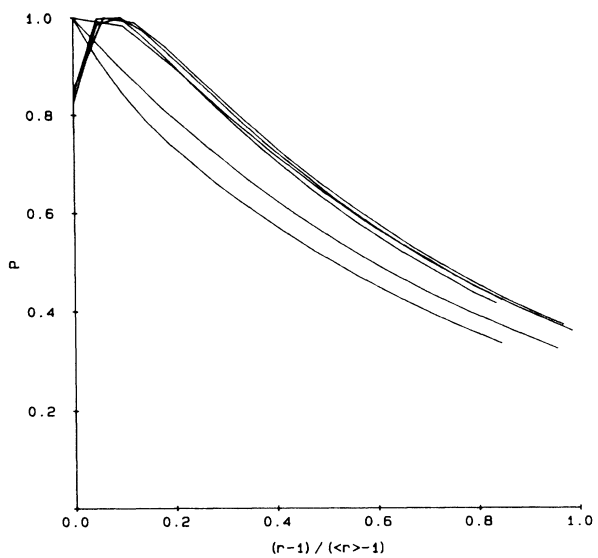

FIG. 9. Linearized NNDD (see text) for three-dimensional $A+A$ and $A+B$ reactions. All curves are for $t=10$ steps, except the $t=0$ (random distribution). Top to bottom (right-hand side): (1) $A+A\rightarrow A$; (2) $A+B\rightarrow 0$, AB NNDD; (3) $A+B\rightarrow 0$, PP NNDD; (4) $A+A\rightarrow 0$; (5) $t=0$, random NNDD; (6) $A+B\rightarrow 0$, AA NNDD. 5000 runs on a $40\times 40\times 40$ cubic lattice with initial density $\rho_0=0.05$ for each component. $\langle r\rangle$ is given by ρ^{-1}.

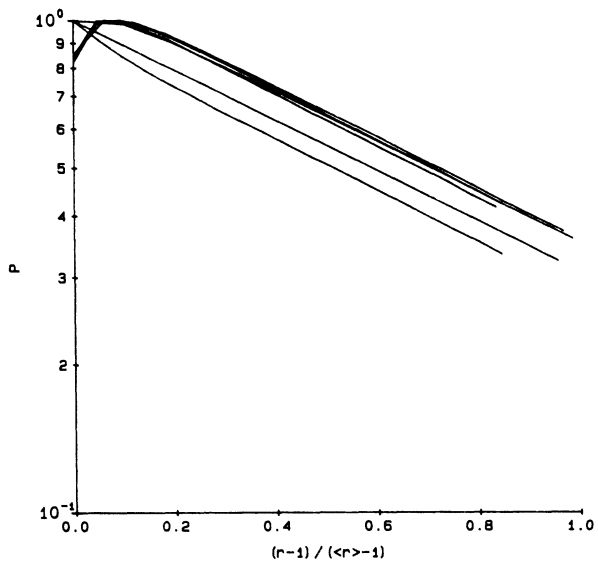

FIG. 10. Semilog plot of Fig. 9 data.

(compare to Figs. 1 and 5). This is also clear from Fig. 8, which demonstrates again that only the overall (PP) NNDD is quasirandom, while the partial (AA and AB) NNDD deviate significantly from a Poissonian form. We note that while this statistical analysis is one dimensional (along the cut), the chemistry (reaction) is still two dimensional, so that there is no reason to expect the one-dimensional kinetics results of Figs. 1 and 2. For comparison purposes, Figs. 7 and 8 include also the $A+A\rightarrow 0$ and $A+A\rightarrow A$ kinetic NNDD curves (compare paper I). Qualitatively these curves again resemble the AB NNDD (compare Figs. 3–5).

Figures 9 and 10 give the linearized NNDD representations of the three-dimensional ($40\times 40\times 40$ cubic lattice) $A+B$ and $A+A$ reactions. The finite size effects are even more severe here. To avoid them in part, the kinetic results are given for $t=10$ (there is little change with larger t). Instead of $\langle r\rangle$, we use here ρ^{-1}. This improves the x-axis normalization, but does not completely correct for the finite size effects. Figure 9, however, suffices to establish the presence of local gaps (black holes) due to the reaction process. These are only of the order of the reaction cross section (a lattice unit), and thus expected from the standard Smoluchowski–de Gennes approach.[10,11] Even the two-dimensional lattice "holes" are not much larger than the reaction cross section. Figures 8 and 10 probe more clearly the potential difference between the two- and three-dimensional kinetics: The deviation from a random (Hertzian) distribution is restricted to very small interparticle distances in three dimensions (this is also true for $t=100$). This is only slightly less true for the two-dimensional lattice (but much less so for the lower dimensions). In addition, there is not much difference between the NNDD of the $A+A$ and those of the $A+B$ reactions. It thus becomes obvious that on the time scale of these kinetic runs, no large-scale (macroscopic) segregation takes place, in contrast to the asymptotic (long-time) results of Ovchinnikov and Zeldovich,[12] Toussaint and Wilcek,[13] and others.[14,15] This is also corroborated by the similar behavior of the $A+A$ reactions, where no segregation is possible. Our interest is thus focused on the microscopic (or mesoscopic) ordering, which obviously does occur.

In summary, we have found interesting empirical correlations among the nearest-neighbor distributions of the $A+A$ and $A+B$ reactions. We hope that this will spur further analytical investigations concerning the spatial distributions of the $A+B$ (and $A+A$) reactions in the short- and medium-time domains in all dimensions.

ACKNOWLEDGMENTS

We thank Eric Clement, Laurel Harmon, Li Li, and Stephen Parus for helpful discussions. This work has been supported by The National Science Foundation Grant No. DMR-8801120 and by the donors of the Petroleum Research Fund, administered by the American Chemical Society.

[1]P. Argyrakis and R. Kopelman, preceding paper, Phys. Rev. A **41**, 2113 (1990).
[2]C. R. Doering and D. ben-Avraham, Phys. Rev. A **38**, 3035 (1988).
[3]P. Argyrakis and R. Kopelman, Phys. Rev. B **31**, 6008 (1985).
[4]R. Kopelman, J. Stat. Phys. **42**, 185 (1986).
[5]E. Horowitz and S. Sahni, *Fundamentals of Computer Algorithms* (Computer Science, Potomac, MD, 1978).

[6]P. Hertz, Math. Ann. **67**, 387 (1909).
[7]E. W. Montroll and W. W. Badger, *Introduction to Quantitative Aspects of Social Phenomena* (Gordon and Breach, New York, 1974), p. 100.
[8]R. Kopelman, S. J. Parus, and J. Prasad, Chem. Phys. **128**, 209 (1988).
[9]G. H. Weiss, R. Kopelman, and S. Havlin, Phys. Rev. A **39**, 466 (1989).
[10]M. V. Smoluchowski, Phys. Z **17**, 585 (1916).
[11]P. G. deGennes, J. Chem. Phys. **76**, 3316 (1982).
[12]A. A. Ovchinnikov and Ya. B. Zeldovich, Chem. Phys. **28**, 215 (1978), and references therein.
[13]D. Toussaint and F. Wilczek, J. Chem. Phys. **78**, 6242 (1983).
[14]K. Kang and S. Redner, Phys. Rev. Lett. **52**, 955 (1984).
[15]P. Meakin and H. E. Stanley, J. Phys. A: Gen. Phys. **17**, L172 (1984).